Spring 4-2014

Synthesis and Characterization of a Tetra-Ruthenated Naphthylbiliverdin

Ashley M. Berding

Synthesis and Characterization of a Tetra-Ruthenated Naphthylbiliverdin

Honors Thesis

Ashley M. Berding

Department: Chemistry

Advisor: Shawn Swavey Ph.D.

April 2014

Synthesis and Characterization of a Tetra-Ruthenated Naphthylbiliverdin

Honors Thesis

Ashley M. Berding

Department: Chemistry

Advisor: Shawn Swavey Ph.D.[a]

April 2014

Abstract:

A new naphtylbiliverdin compound has been synthesized which offers intense absorption with the photodynamic therapy window (600 nm – 850 nm). The compound has been characterized by proton NMR, high resolution electrospray mass spectrometry, elemental analysis, and UV/vis spectroscopy. Coordination of four ruthenium(II) polypyridyl complexes was accomplished by standard procedures. The new tetra-ruthenated naphthylbiliverdin was characterized by elemental analysis. Cyclic voltammetry measurements reveal that all four ruthenium moieties are coordinated to the pyridyl groups of the biliverdin compound. The intense metal to ligand charge transfer (MLCT) bands of the peripheral ruthenium groups overshadow the absorption due to the biliverdin compound; therefore, spectroelectrochemical studies were conducted to show that the low energy absorption of the naphthylbiliverdin compound is unaffected by coordination to the ruthenium groups. DNA photocleavage studies were performed by irradiating samples containing plasmid DNA and the ruthenated compound, filtering out high energy light. Gel electrophoresis studies indicate that the compound is capable of photonicking the plasmid DNA when irradiated with light.

[a] *Department of Chemistry, University of Dayton, 300 College Park, Dayton, OH. 45469-2357.*

*To whom correspondence should be addressed.
Telephone: 1-937-229-3145. Fax: 1-937-229-2635.
E-mail: sswavey1@udayton.edu.

Table of Contents

Introduction

I. Photodynamic Therapy

Photodynamic therapy is the use of light, molecular oxygen, and a photosensitizer to destroy tumor cells. In 1900, Oskar Raab discovered photodynamic therapy[1] when he used acridine orange and light to destroy living organisms. This therapeutic use of light was further investigated and it was found by Policard that fluorescence was more targeted toward tumor cells than normal healthy tissue.[2] Gaining this insight led to development of photodynamic agents which were used to treat bacterial infections[3] and inflammation.[4] Tumor specificity of photodynamic therapy agents also led to treatment of bladder cancers, brain cancers, breast metastases, skin cancers, gynecological malignancies, colorectal cancers, thoracic malignancies, oral cancers, and neck cancers.[5]

For reasons not completely understood, photodynamic therapy causes immune system suppression along with the cancer cell death.[6] Korbelik[7] has studied the mechanism associated with immune system suppression associated with PDT and has found that tissues which are treated in PDT release large amounts of cell debris, inflammatory signals, cytokines, and chemo-tactic agents which cause the tissue to secrete immunosuppressive signals leading to the immuno-depression in the cell.

II. Mechanisms

As stated earlier, photodynamic therapy is the use of therapeutic light, molecular oxygen, and a photosensitizer to destroy cancerous cells in a multitude of different diseases. This route of treatment is a more targeted and less invasive approach than other methods such as surgery or chemotherapy and comes with little side effects. There are two different mechanisms that explain the destruction of tumor cells in photodynamic therapy, both which start by excitation of a photosensitizer with light.[8]

Excitation of the photosensitizer causes promotion of an electron to a higher energy state. In the Type I mechanism, the excited photosensitizer goes on to react with molecular oxygen to give the superoxide radical (illustrated in Scheme 1) which can go on to form hydroxyl radicals ($OH^{\bullet}$) which are extremely toxic and lethal to the cell. The Type I mechanism is dependent on the target substrate concentration in the cell. A reaction which is less likely to occur but is thought to happen in anoxic environments is when the excited photosensitizer reacts directly with an organic substrate by electron exchange. This electron exchange, usually with guanine of the DNA which is most easily oxidized, fills the hole on the photosensitizer which was left empty during excitation.[9] Oxidation of the guanine causes destruction of the DNA thus promoting apoptosis.

Scheme 1: Photodynamic Therapy Mechanisms

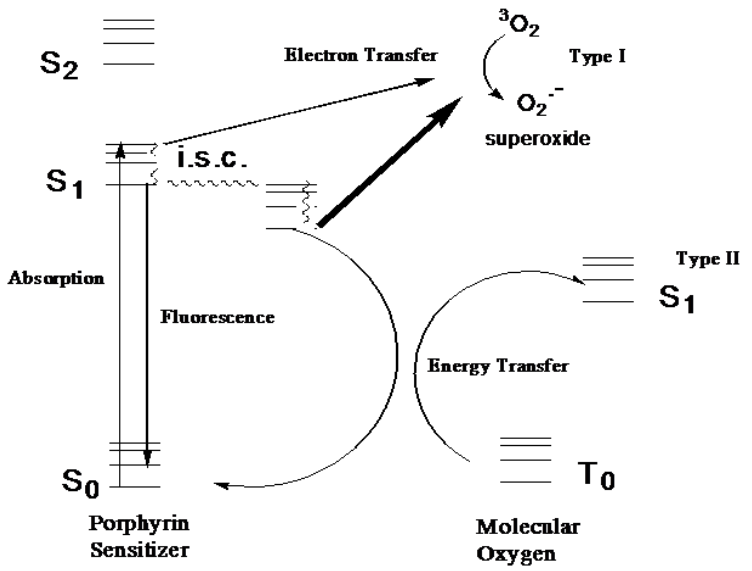

The Type II mechanism also involves excitation of a photosensitizer with light but it transfers energy to the ground state of oxygen changing triplet state oxygen into the more reactive singlet state oxygen (Scheme 1). Oxygen in the singlet state is now able to go on and destroy cellular function by reacting with various portions of the cell.[10] Oxygen is unique in that it has low lying excited states and the energy required to transition into the excited state is also low.[11] This Type II mechanism is thought to be the main mechanism of photodynamic therapy in cells and is characterized by a dependence on oxygen concentration within the cell.[12]

The first compound used as a photosensitizer for photodynamic therapy was a hematoporphyrin derivative which was later purified and is marketed as Photofrin®. It has been authorized to treat lung and esophageal cancers along with dysplasia.[13] Photofrin®, Figure 1, a purified version of the hematoporphyrin derivative was first discovered in the 1970's. It's use as a

photosensitizer in PDT is to create singlet state oxygen from triplet state oxygen upon photoexcitation in the visible region of the spectrum.[14] Unfortunately, Photofrin® is not efficient at forming singlet oxygen and therefore patients have to stay out of the light for several hours after treatment. In addition Photofrin® is extremely difficult to purify.[15-18]

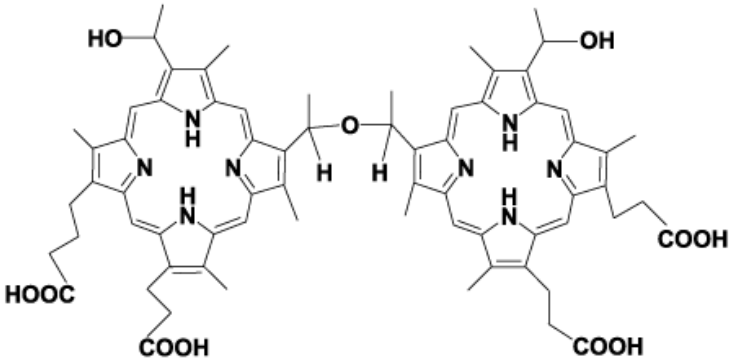

Figure 1: Photofrin®

III. Porphyrins as Photosensitizers

Porphyrins have, for many years, been studied for their capabilities as PDT agents due to their planar aromatic structure, photophysical properties, and straight forward synthesis.[19-23] The general synthesis of a porphyrin and a metalloporphyrin requires the reaction of a pyrrole and an aldehyde, shown below in Figure 2, and then further purification using column chromatography. The spectroscopic properties of these compounds are characterized by intense absorptions near 400 nm (the Soret band) with molar absorptivities in the hundreds of thousands and less intense Q-bands ranging from 500 nm to 700 nm. For the greatest penetration of light through human tissue there exists a photodynamic therapy window which lies between 600 nm and 850 nm; since the lower energy Q-bands of the porphyrin are located

near 650 nm these are the bands of interest for PDT. Unfortunately, due to the relatively low molar absorptivities of these Q-bands they suffer from the same problem as Photofrin and are not able to efficiently generate singlet oxygen within the PDT window.

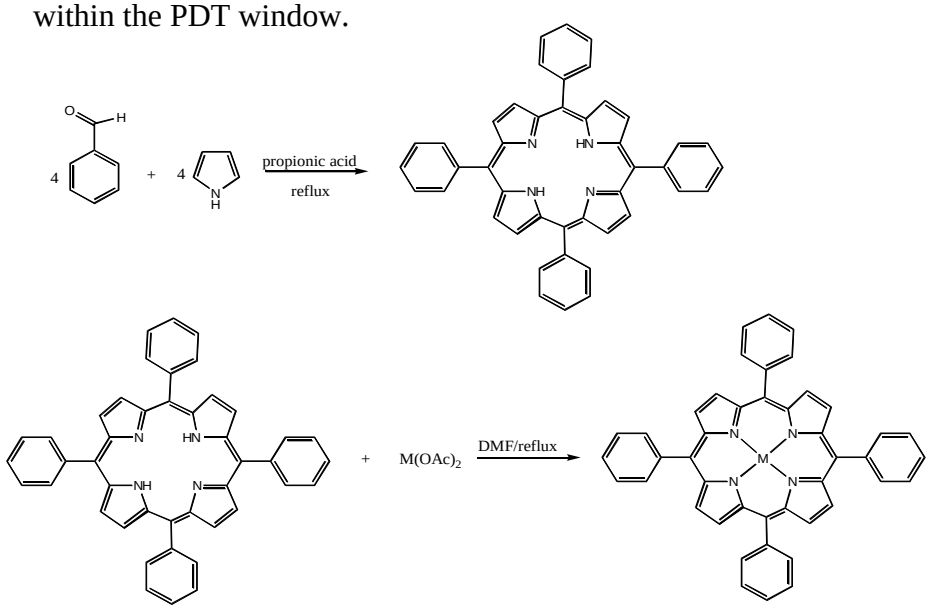

Figure 2: Synthesis of Porphyrin and Metalloporphyrin

Another issue associated with porphyrins is their lack of water solubility. Cationic porphyrins have been studied to try and solve this issue because they tend to be more water soluble and also have strong electrostatic interactions with the negatively charged DNA backbone.[24] Other examples of synthetically modified porphyrins include halogenated porphyrins which have extend excited state lifetimes resulting in greater singlet oxygen formation.[25-28] It was found that by covalently binding halogens to the meso-positions, the excited state lifetime is significantly longer than in un-halogenated analogs.[25]

Ruthenium complexes containing polypyridyl ligands have also been synthesized for the Metal to Ligand Charge Transfer (MLCT) state of the ruthenium that is proven to lead to formation of reactive oxygen species which have the ability to cleave supercoiled DNA.[29] Our choice to use ruthenium polypyridyl moieties as pendant groups stems from the initial work of Araki, Toma and coworkers, as seen below in Figure 3.

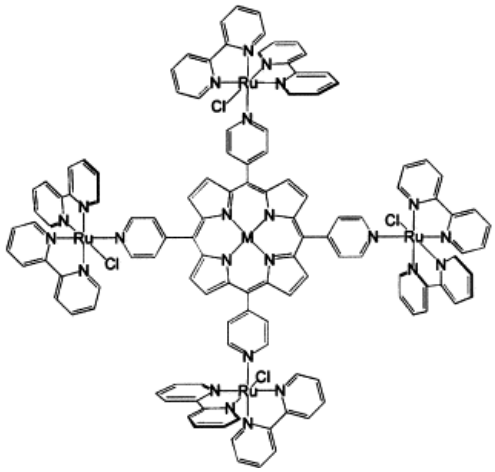

Figure 3: Structural representation of $[TPyP\{Ru(bipy)_2Cl\}_4]^{4+}$ complex, TRP.[30]

Recently, a number of groups have explored the synthetic possibilities of shifting the Soret band further into the visible region of the spectrum. This has been accomplished, in large part, by extending the conjugation of the pyrrole groups leading to porphyrins with Soret bands shifted to 550 nm and greater.[31] Unfortunately, due to synthetic limitations the majority of these new porphyrins are not water soluble, limiting their applications.

Oxidation of porphyrins to biliverdins has recently received a great deal of attention. These linear tetrapyrroles can play important roles in molecular electronics and liquid crystals.[32] Numerous methods have been used to

facilitate the formation of biliverdins from porphyrins such as photochemical oxidation, chemical oxidation, and coupled oxidation.[33-35] In biological systems degradation of heme occurs in the spleen by the enzyme heme oxygenase converting the heme to biliverdin.

In our attempt to make a π-extended naphtylporphyrin containing peripheral coordination sites we have unexpectedly isolated a new type of biliverdin with long wave excitation and fluorescence properties. These complexes have been investigated for their electrochemical and spectroscopic properties. In addition, insertion of transition metal ions into the porphyrin core resulted in catalytic and small molecule detection applications. Irradiation of solutions of the free base tetra-ruthenated porphyrin and plasmid DNA resulted in single strand breaks.[30] Since this work, numerous ruthenated porphyrin complexes have been studied as potential photodynamic therapy agents. Herein we present our attempt to create a tetra-pyridyl porphyrin with extended conjugation of the pyrrole units capable of coordinating four $[Ru(bpy)_2Cl]^+$ moieties.

Experimental

I. Materials

1-nitronapthalene (Acros), tetrahydrofuran (Acros), ethyl isocyanoacetate (Acros), phosphazene base (Aldrich), dichloromethane (VWR), sodium sulfate (Fisher), silica gel (Fisher), methanol (Fisher), acetone (Fisher), toluene (Fisher), potassium hydroxide (Fisher), ethylene glycol (Acros), hydrazine (Aldrich), propionic acid (Acros), ammonium hydroxide (Acros), chloroform (Fisher), glacial acetic acid (Fisher), acetonitrile (VWR), used for electrochemistry, and tetra-n-butyl ammonium hexafluorophosphate (Bu_4NPF_6, used as supporting electrolyte for electrochemistry, Acros) were used without further purification. *cis*-$Ru(bipy)_2Cl_2$ was synthesized as previously described.[36] The plasmid, pUC18, was obtained from Buyou Biolabs. Electrophoresis-grade low EEO agarose, tris base, sodium chloride and boric acid were obtained from Fisher. Ethidium bromide was obtained from EM Science. The spectroscopic titration was carried out at room temperature in the buffer (5 mM Tris-HCl, 0.1 mM NaCl, pH 7.2). Concentration of calf thymus DNA (Sigma) solution used in the titrations was determined spectrophotometrically using the extinction coefficient 6600 M^{-1} cm-1 at 260 nm.[37] The photocleavage studies were carried out in room temperature using buffer (0.44 M Tris base, 0.44 M Boric acid). All aqueous solutions were prepared using doubly distilled water. Elemental analysis was performed by Atlantic Microlab, Norcross, Ga. High resolution electrospray

mass spectrometry was performed by the Ohio State mass spectrometry and proteomics facility, Columbus, OH.

II. Synthesis

Naphthylpyrrole Ester

The naphthylpyrrole ester was synthesized as previously described.[38] To a solution of 2.30 g (13.3 mmol) of 1-Nitronapthalene in 100 mL of dry THF was added 2.00 g (17.7 mmol) of ethyl isocyanoacetate and 4.20 mL (13.7 mmol) of phosphazene base. The solution was refluxed overnight upon which, after cooling to room temperature, the solution was diluted with dichloromethane, washed with water, and dried over sodium sulfate. After removing the solvent under reduced pressure the brown powder was chromatographed on silica gel using dichloromethane as eluent. After the first orange band was collected the solvent was switched to 1% methanol to collect the product as a pale yellow compound. Recrystallization from hot toluene gave the final peach colored product.

Naphthylpyrrole

To a solution of 1.5 grams of potassium hydroxide in 20 mL of ethylene glycol was added 0.43 g (1.8 mmol) of the naphthylpyrrole ethylester. The solution was purged with nitrogen for 20 min and 10 drops of hydrazine was added. After reflux for 30 min under nitrogen the solution was added to an ice/water mixture resulting in a gray precipitate. The precipitate was filtered, washed with water and air dried overnight to give a yield of 0.22 g.

Naphthylbiliverdin

A 75 mL solution of propionic acid containing 2.7 grams (0.016 moles) of naphthylpyrrole and 1.7 g (0.016 moles) of 4-pyridine carboxaldehyde was refluxed for1 h. After cooling to room temperature, 50.0 mL of methanol was added. This was then neutralized with 150 mL of 50:50 methanol/NH_4OH solution. The precipitate was filtered and air dried overnight. Chromatography was performed using silica gel with choloform followed by a 1% methanol/$CHCl_3$ to collect the first band. This was followed by a 2% methanol/$CHCl_3$ to collect the second band and then finally a 5% methanol solution to collect the last purple band yielding 75 mg of product. Anal. Calc. for $C_{72}H_{42}N_8O_2 \cdot 4H_2O$: C, 77.06; H, 4.40; N, 9.99, Found: C, 76.74; H, 4.10; N, 9.80; TOF MS ES+ m/z 1052 ($M+H^+$).

Tetra-ruthenated naphthylbiliverdin

Under a nitrogen atmosphere 20 mg (0.02 mmol) of naphthylbiliverdin and 38 mg (0.08 mmol) of *cis*-$Ru(bipy)_2Cl_2$ were refluxed in 15 mL of glacial acetic acid for 45 minutes. The solvent was removed and approximately 5 mL of methanol was added and refluxed under N_2 gas for an additional 30 minutes. The solution was added drop-wise to an aqueous saturated ammonium hexafluorophosphate solution, the precipitate was filtered, washed with water, and air dried to yield 56 mg. Anal. Calc. for $C_{152}H_{106}N_{24}O_2Cl_4P_4F_{24}Ru_4 \cdot 8H_2O$: C, 51.12; H, 3.44; N, 9.41; F, 12.77, Found: C, 51.39; H, 3.28; N, 9.32; F, 12.38.

III. Measurements

Electronic Spectroscopy

UV/Vis spectra were recorded for all three compounds at room temperature using an HP-8453 photodiode array spectrophotometer with 2 nm resolution. Samples were run in acetonitrile in 1 cm quartz cuvettes.

Electrochemistry

Solution cyclic voltammograms were recorded using a one-compartment, three electrode cell (model 630A Electrochemical analyzer from CH-Instruments) equipped with a platinum wire auxiliary electrode. The working electrode was a 2.0 mm diameter glassy carbon electrode from CH-Instruments. The working electrode was polished first using 0.30 μ followed by 0.05 μ alumina polish (Buehler), then sonicated for 20 sec. and tapped dry with a kimwipe prior to use. Potentials were referenced to a silver/silver chloride electrode(Ag/AgCl). The supporting electrolyte was 0.1 M Bu_4NPF_6 and the measurements were made in extra dry acetonitrile.

Spectroelectrochemistry

A spectroelectrochemical analysis of the ruthenated porphyrin was conducted according to a previously described method with a locally constructed H-cell which uses a quartz cuvette as the working compartment.[39] The working and auxillary compartments of the H-cell were separated by a glass frit. The potetials were referenced versus a Ag/AgCl electrode, a platinum wire served as the auxillary electrode and a high surface area platinum mesh served as the working electrode. The solution contained 0.1 M Bu_4NPF_6 as the supporting

electrolyte and all measurements were made in acetonitrile. A CH-Instruments 630A electrochemical analyzer controlled the electrolysis potential.

DNA Titrations

DNA titrations of the three compounds were conducted using an HP-8453 photodiode array spectrophotometer with 2 nm resolution. A 1 cm quartz cuvette was filled with 3 mL of the ruthenated compound for initial analysis under UV/Vis and subsequent 5 μL aliquots of calf thymus DNA in buffer (5 mM Tris-HCl, 0.1 mM NaCl, pH 7.2) were added up to 100 μL of DNA.

Photocleavage

Photocleavage of the ruthenated compound was conducted using buffer (0.4 M Tris base, 0.4 M Boric acid) combined with pUC18 at a ratio of 10:1 bp: complex in a 500 μL quartz cuvette. The cuvette was irradiated under visible light using a 420 nm cutoff filter with a 300 W mercury arc lamp. At 10, 20, 30, 40, 50, 60, 70, and 80 minute time intervals samples of the solutions were removed and run on a 0.8% agarose gel by applying 226 V for 45 minutes in approximately 500 mL of Tris buffer solution. The gels were stained with ethidium bromide and photographed using UV illumination.

Results and Discussion

I. Synthesis and characterization

To simultaneously allow for coordination of ruthenium polypyridyl moieties and incorporate water solubility to a highly conjugated porphyrin, 4-pyridine carboxaldehyde was chosen for the meso-substituent. Understanding that the Lindsey method[40] has limited success when heterocyclic aldehydes are used[41-43] we opted to use the Adler-Longo[44] synthetic route. Since this method typically results in low yields it was necessary to use larger quantities of starting reagents. Gram quantities of naphtha[1,2-c]pyrrole[41-43] and 4-pyridine carboxaldehyde were subsequently refluxed in propionic acid and neutralized with an ammonium hydroxide/methanol solution. Further purification yielded a bright purple powder with an intense band at ca. 560 nm in the electronic absorption spectrum. We were puzzled however by the absence of Q-bands. Further analysis of the compound using soft ionization mass spectroscopy (TOF MS ES+) gave an $[M-H]^+$ of 1052. The MS data along with elemental analysis and ^{1}H NMR led us to the proposed structure given in Scheme 2.

Scheme 2. Synthesis of naphthylbiliverdin.

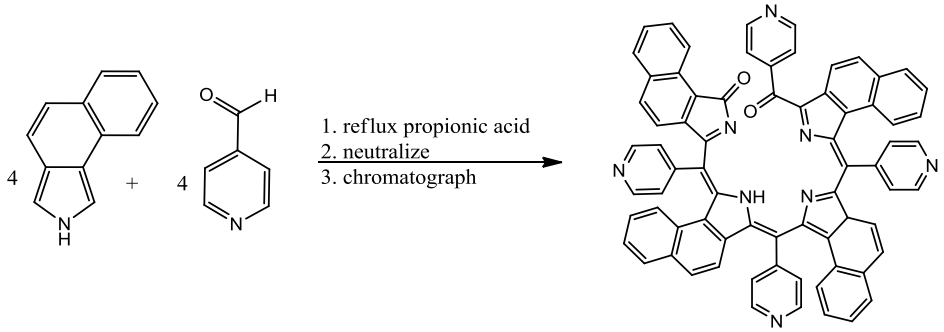

Although not the target porphyrin we had anticipated, we were able to successfully coordinate $[Ru(bpy)_2Cl]^+$ to the pyridyl nitrogens to give complex I seen in Figure 4 below.

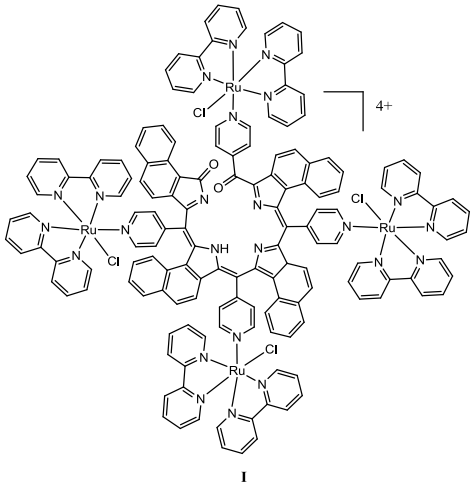

I

Figure 4: [complex I]

Electronic absorption spectra of naphthylbiliverdin and its ruthenated analog (I) was run in acetonitrile solutions, Fig. 5. A broad absorption band with λ_{max} of 560 nm is observed for biliverdin compound with a molar absorptivity of ca. 34,000 $M^{-1}cm^{-1}$, blue line Fig. 5, associated with π-π* transitions.

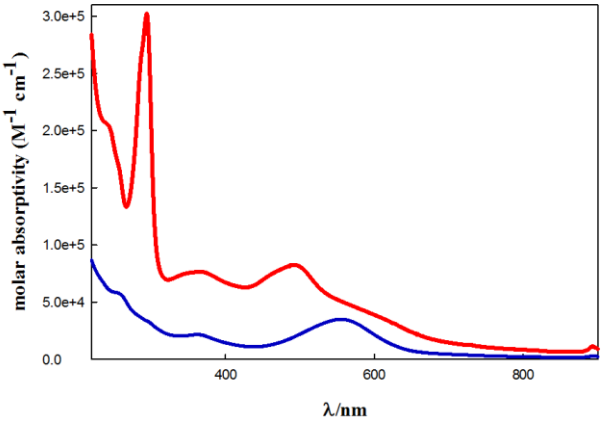

Figure 5. UV/vis spectra of naphthylbiliverdin, blue line, and I, red line, in acetonitrile.

The ruthenated complex (I), red line Fig. 5, displays an intense absorption band at 295 nm associated with π-π* transitions of the bipyridyl groups. Two less intense bands at 366 nm and 493 nm are attributed to the Ru(dπ)-bpy(π*) metal to ligand charge transfer (MLCT) transitions. A slight shoulder red-shifted from the 493 nm absorption band is believed to be the result of the underlying π-π* transitions of biliverdin core. Solution phase cyclic voltammetry (CV) in dry acetonitrile containing $TBAPF_6$ as supporting electrolyte was performed using a three electrode system with a glassy carbon working electrode. Figure 6 illustrates the results of this study where Fig. 6A represents the cyclic voltammogram of TPyTNP and Fig. 6B represents the cyclic voltammogram of complex **I**.

When the TPyTNP solution is cycled in the cathodic direction there is an irreversible reduction process at -0.74 V versus Ag/AgCl which is due to reduction of the ligand, further cathodic scanning led to a sharp irreversible reduction wave nearly off scale (not shown). It is unclear what this wave represents, possibly surface polymerization. In the anodic direction there is evidence for an irreversible oxidation wave at approximately 1.40 V versus Ag/AgCl. Solution cyclic voltammetry of complex I, Fig. 6B, shows two irreversible reduction waves at -0.28 V and -0.69 V versus Ag/AgCl and a reversible redox couple with $E_{1/2}$ = 0.87 V (ΔE = 70 mV) associated with the Ru(III/II) couple. This represents a shift of ca. 0.40 V when compared to the $Ru(bpy)_2Cl_2$ starting material indicative of the stabilization of the t_{2g} orbitals of Ru upon replacing a π-donor ligand (Cl^-) with a π-acceptor ligand (pyridine) thus

indicating that the ruthenium is indeed coordinated to the pyridyl groups of TPyTNP.

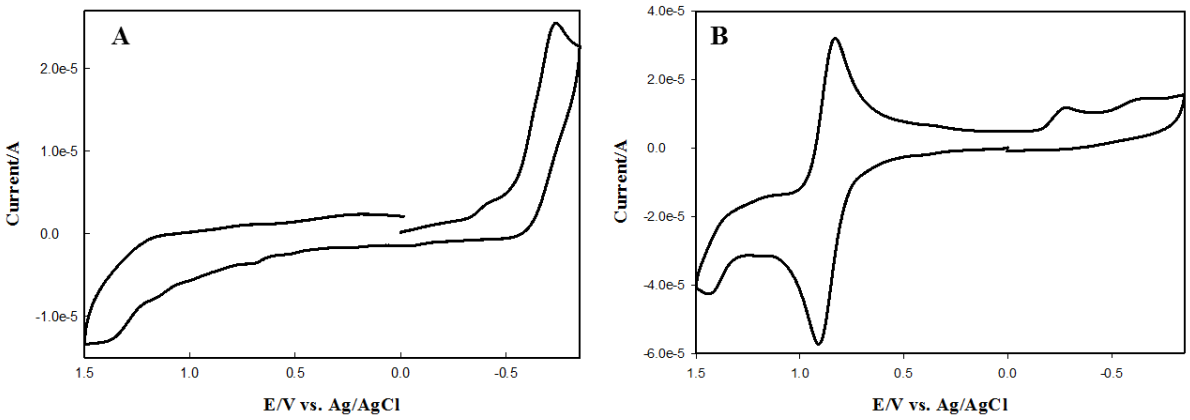

Figure 6. Cyclic voltammograms of TPyTNP, A, and complex I, B, in 0.1 M $TBAPF_6$/acetonitrile at room temperature. ν = 100 mV/s, N_2 atmosphere.

To help determine if the absorption band observed for TPyTNP at ca. 560 nm is present in the ruthenated complex (I) spectroelectrochemistry was performed. Electrolysis of a solution of I at a potential of 1.20 V versus Ag/AgCl oxidized the Ru(II) to Ru(III) thus decreasing the Ru(dπ) to bpy(π*) MLCT transition without effecting the TPyTNP. Figure 7 illustrates the spectroscopic results of the oxidative electrolysis of a solution of I in acetonitrile solution. As the potential is applied the MLCT transition at 493 nm begins to decrease. A new band at 595 nm begins to appear, associated with the absorption of the TPyTNP ligand. The new transition is shifted to the red by 35 nm compared to the free TPyTNP absorption band, Fig. 5 blue line. This is in agreement with the positive shift observed in the reduction of TPyTNP of complex I from -0.74 V for the free TPyTNP (Fig. 6A) to -0.69 V for complex I (Fig. 6B) resulting from stabilization of the TPyTNP π* orbitals upon coordination of the Ru(II) moiety.

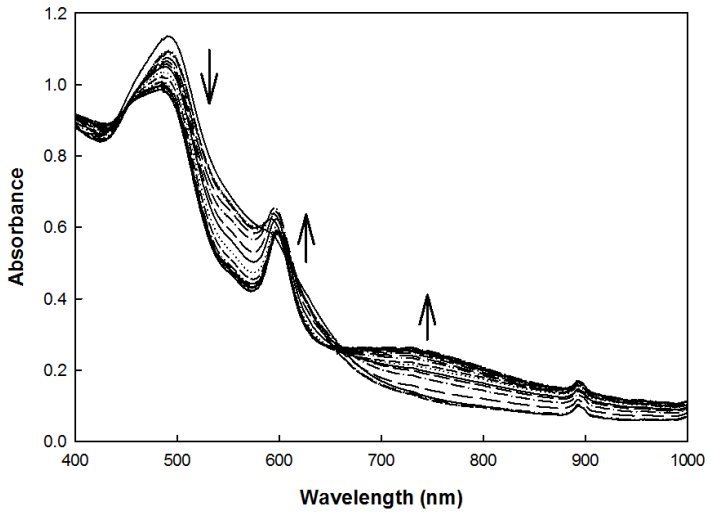

Figure 7. Spectroelectrochemistry complex I in 0.1 M $TBAPF_6$ acetonitrile at room temperature. Electrolysis performed at 1.20 V vs. Ag/AgCl.

In addition an isosbestic point at ca. 665 nm is observed with an increase of a broad shoulder at 745 nm indicative of only two species in solution (i.e. Ru(II) complex I and Ru(III) complex I).

II. DNA binding

To determine quantitatively a binding constant for the interaction of complex I with DNA absorption titrations were used. Aqueous solutions of constant [complex I] were titrated with pH 7 buffered solutions of calf thymus (CT) DNA, the titrations were run in triplicate. Figure 8 illustrates the effects of additions of CT-DNA on the absorbance of the MLCT transition at 493 nm for complex I. The MLCT transition decreases as the concentration of CT-DNA increases indicating an interaction between complex I and CT-DNA. The intrinsic binding constant K_b for the CT-DNA complex I interaction was determined from equation 1:[45]

$$[DNA]/(\varepsilon_a-\varepsilon_f) = [DNA]/(\varepsilon_b-\varepsilon_f) + 1/K_b(\varepsilon_b-\varepsilon_f) \qquad \text{eq. 1}$$

where ε_a = absorbance/[complex I], ε_b and ε_f are the extinction coefficients for the fully bound and free form of complex I respectively. A linear fit of the plot (inset Fig.8) of $[DNA]/(\varepsilon_a-\varepsilon_f)$ versus [DNA] gives a slope of $1/(\varepsilon_b-\varepsilon_f)$ and an intercept of $1/K_b(\varepsilon_b-\varepsilon_f)$. A value of $K_b = 6.0 \times 10^5\ M^{-1}$ was determined by this method. The magnitude of K_b suggest and intercalative process for the binding of complex I with DNA.[46]

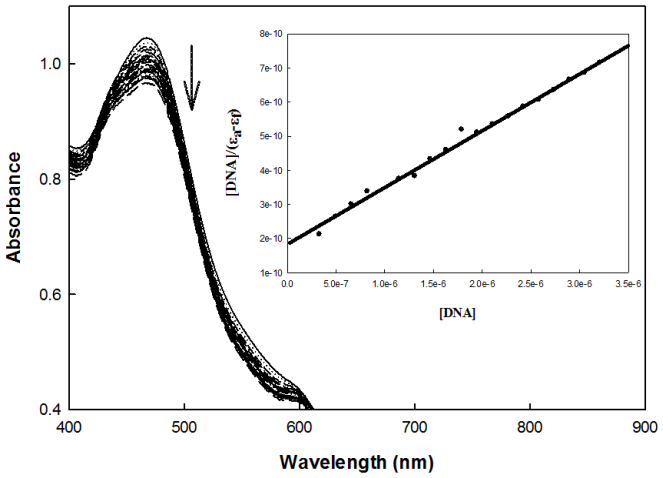

Figure 8. Absorption spectra of complex I in the presence of increasing amounts of CT-DNA [Complex I] = 20 μM, [DNA] = 0 –3.1μM.

I. DNA photoreactions

When buffered, pH 7, solutions of circular plasmid DNA (pUC18) containing complex I, in a ratio of 10:1 bp:complex I, are irradiated with a 300 W mercury arc lamp, filtered to allow only light of 420 nm and higher to penetrate the solution, the supercoiled DNA is converted to nicked circular DNA, Figure 9.

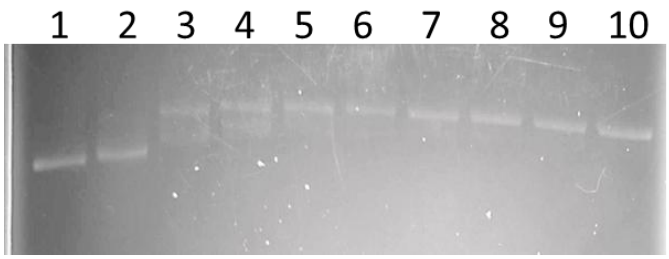

Figure 9. Gel electrophoresis of circular plasmid DNA (pUC18) in the presence of complex I (lanes 2-10) and without complex I (lane 1) irradiated with a 300 W mercury arc lamp filtered to allow only light of 420 nm and higher to penetrate. Samples taken at 10 min intervals.

Lane 1 represents the plasmid DNA without complex. Lane 2 represents a solution of plasmid DNA and complex I prior to irradiation. Lanes 3-10 represent plamid DNA and complex I with irradiation; samples were taken at 10 minute intervals. Lane 3 indicates that after only 10 min of irradiation the majority of the plasmid DNA has been photonicked. After 30 min all of the plasmid DNA has been photonicked, lane 5 Fig. 9. Further irradiation does not result in complete photocleavage of the plasmid DNA. Similar experiments were run with a 550 nm filter, allowing only light of 550 nm or higher to penetrate the solution, with no effect on the plasmid DNA. We had expected that due to the intense absorption of the TPyTNP ligand at greater than 550 nm photonicking of the plasmid DNA would occur.

Conclusion

In this study, a tetra-ruthenated billiverdin was synthesized and characterized. Synthesis of the complex was done using the Adler-Longo process and subsequent coordination of ruthenium complexes was completed using previously synthesized *cis*-$Ru(bipy)_2Cl_2$. This newly created tetra-ruthenated billiverdin was characterized and the structure was verified through UV/VIS spectroscopy, cyclic voltametry, electrolysis, and mass spectrometry. DNA titration studies indicate that this compound is able to bind to DNA through intercalation with the DNA backbone. Photocleavage studies of this compound indicate that through photonicking, the compound is able to effectively cleave the DNA which suggests the potential of the compound as candidate for cell destruction.

Further direction of this research will include re-synthesis of the billiverdin complex for verification of the methods used. The complex will also be analyzed for verification of characterization. Once the billiverdin structure is confirmed, it will again be tested for it's ability to bind and then cleave DNA. The hypothesis for this experiment using the billiverdin without the ruthenium groups is that the billiverdin will be able to more effectively cleave DNA within the photodynamic window.

References

1. O. Raab. *Z. Biol.* 1900, **39**, 524.
2. A. Policard. *Compt. Rend. Soc. Biol.*, 1924, **91**, 1423.
3. R.A. Neurath, N. Strick, A.K. Cebinath, *J. Mol. Recog*., 1995, **8**, 345.
4. K.S. McMahon, T.J. Wieman, P.H. Moore, V.H. Fingar. *Cancer Res*., 1994, **54**, 5374.
5. (a) T.J. Dougherty, C.J. Gomer, B.W. Henderson et al. *J. Natl. Cancer Inst.* 1998, **90**, 889. (b) R.K. Pandey, G. Zheng. *Porphyrins as Photosensitizers in Photodynamic Therapy*. Vol. 6. Kadish, Smith, Guilard. (eds). Academic Press:San Diego., 2000.
6. R.K Pandey, *J. Porph. Phthalocyan.*, 2000, **4**, 368.
7. M. Korbelik. *J. Clin. Laser Med. Surg*. 1996, **14**, 329.
8. J.-L. Ravanant, T. Douki, J.J. Cadet, *Photochem. Photobiol. B*., 2001, **63**, 88.
9. A. Belvedere, F. Bosca, A. Catalfo, M.C. Cuquerella, G. de Guidi, M.A. Miranda, *Chem. Res. Toxicol*., 2002, **15**, 1142.
10. K.R. Weishaupt, C.J. Gomer, T.J. Dougherty. *Cancer Res*., 1976, **36**, 2326.
11. C.S. Foote. Mechanisms of photo-oxygenation. In *Porphyrin Localization and Treatment of Tumors*. Doiron DR, Gomer CJ. (eds). Alan R. Liss: New York, 1984, 3 – 18.
12. F.H.J. Figge. The relationship of pyrrol compounds to carcinogenesis. In *AAAS Research Conf. on Cancer*. F.R. Moulton. (eds). 1945, 117 – 128.
13. T.J. Dougherty. J. *Clin Laser Med. Surg*., 1996, **14**, 219.
14. T.J. Dougherty. J. *Natl. Cancer Inst.*, 1974, **52**, 1333.
15. K.E. Erkkila, D.T. Odom, J.K. Barton, *Chem. Rev*. 1999, **99,** 2777.
16. (a) P.M. Armistead and H.H. Thorp, *Anal. Chem.* 2001, **73,** 558. (b) I.V. Yang and H.H. Thorp, *Inorg. Chem*. 2000, **39**, 4969. (c) P.J. Carter, C.-C. Cheng, H.H. Thorp, J. *Am. Chem. Soc.* 1998, **120**, 632. (d) C. Vialas, C. Claparols, G. Pratviel, B. Maunier, J. *Am. Chem. Soc.* 2000, **122,** 2157.
17. T.N. Singh and C. Turro, *Inorg. Chem*. 2004, **43**, 7260.
18. Y.J. Ko, K.J. Yun, M.S. Kang, J. Park, K.T. Lee, S.B. Park, J.H. Shin, *Bioorg. Med. Chem. Lett.* 2007, **17,** 2789.
19. R.K. Pandey, *J. Porph. Phthal* 2000, **4**, 368.
20. R. Hudson, R.W. Boyle, *J. Porph. Phthal.* 2004, **8**, 954.
21. W.H. Wei, Z. Wang, T. Mizuno, C. Cortez, L. Fu, M. Sirisawad, L. Naumovski, D. Madga, J.L. Sessler, *Dalton Trans*. 2006, 1934.
22. X. Chen, C.M. Drain, *Drug Design Rev.* 2004, **1**, 215.
23. R. Allison, H. Mota, C. Sibata, *Photodiagnosis and Photodynamic* Therapy 2004, **1**, 263.
24. J. Onuki, A.V. Ribas, M.H.G. Medeiros, K. Araki, H.E. Toma, L.H. Catalini, P. Di Mascio, *Photochem. Photobiol.* 1996, **63**, 272.

25. S.I. Yang, J. Seth, J.P. Strachan, S. Gentemann, D. Kim, D. Holten, J.S. Lindsey, D.F. Bocian, *J. Porph. And Phtha*l. 1999, **3**, 117.
26. X. Chen, L. Hui, D.A. Foster, C.M. Drain, *Biochem.* 2004, **43,** 10918.
27. Y.J. Ko, K.J. Yun, M.S. Kang, J. Park, K.T. Lee, S.B. Park, J.H. Shin, *Bioorg. Med. Chem. Lett*. 2007, **17**, 2789.
28. X. Zheng, and R.K. Pandey, *Anti Cancer Agents in Med. Chem.* 2008, **8**, 241.
29. M.T. Mangelli, J. Heinceke, S. Mayfield, B. Okyere, B.S.J. Winkel, K.J. Brewer, J. *Inorg. Biochem*. 2006, **100**, 183.
30. H. Toma, K. Araki, *Coordination Chemistry Review* 2000, **196,** 307-329.
31. K. Graham, Y. Yang, J. Sommer, A. Shelton, K. Schanze, J. Xue, J. Reynolds, *Chem. Mater*. 2011, **24**, 5305-5312.
32. N. Asano, S. Uemura, T. Kinugawa, H. Akasaka, T. Mizutani. *J. Org. Chem.*, 2007, **72** (14), 5320–5326
33. (a) Cavaleiro, J. A. S.; Neves, M. G. P. S.; Hewlins, M. J. E.; Jackson, A. H. J. *Chem. Soc., Perkin Trans. 1* 1990, 1937. (b) Cavaleiro, J. A. S.; Hewlins, M. J. E.; Jackson, A. H.; Neves, M. G. P. M. S. *Tetrahedron Lett*. 1992, **33**, 6871. (c) Silva, A. M. S.; Neves, M. G. P. M. S.; Martins, R. R. L.; Cavaleiro, J. A. S.; Boschi, T.; Tagliatesta, P. J. *Porphyrins Phthalocyanines* 1998, 2, **45**. (d) Jeandon, C.; Krattinger, B.; Ruppert, R.; Callot, H. J. *Inorg. Chem.* 2001, **40**, 3149. (e) Bonnett, R.; Martinez, G. *Tetrahedron* 2001, **57**, 9513.
34. (a) Evans, B.; Smith, K. M.; Cavaleiro, J. A. S. J. *Chem. Soc., Perkin Trans. 1* 1978, 768. (b) Ongayi, O.; Vicente, M. G. H.; Ou, Z.; Kadish, K. M.; Kumar, M. R.; Fronczek, F. R.; Smith, K. M. *Inorg. Chem*. 2006, **45**, 1463.
35. (a) Bonnett, R.; Dimsdale, M. J. *Tetrahedron Lett.* 1968, **9**, 731. (b)Bonnett, R.; Dimsdale, M. J. J. *Chem. Soc., Perkin Trans.* 1 1972, 2540.(c) Bonnett, R.; McDonagh, A. F. J. Chem. Soc., *Perkin Trans. 1* 1973, 881. (d) Balch, A. L.; Latos-Grazynski, L.; Noll, B. C.; Olmstead, M. M.; Szterenberg, L.; Safari, N. J. *Am. Chem. Soc.* 1993, **115**, 1422. (e) Balch, A. L.; Latos-Grazynski, L.; Noll, B. C.; Olmstead, M. M.; Safari, N. J. *Am. Chem. Soc.* 1993, **115,** 9056. (f) Morishima, I.; Fujii, H.; Shiro, Y.; Sano, S. *Inorg. Chem*. 1995, **34**, 1528. (g) Johnson, J. A.; Olmstead, M. M.; Balch, A. L. *Inorg. Chem.* 1999, **38**, 5379.
36. B.P. Sullivan, D.J. Salmon, T.J. Meyer, *Inorg. Chem*. 1978, **17**, 3334.
37. M.F. Reichmann, S.A. Rice, C.A. Thomas, P. Doty, J. *Am. Chem. Soc*. 1954, **76**, 3047.
38. T. Lash, M. Thompson, T. Werner, J. Spence, *Synlett* 2000, **2**, 213-216.
39. K.J. Brewer, M. Calvin, R.S. Lumpkin, J.W. Otvos, O.L. Spreer, *Inorg. Chem.* 1989, **28**, 4446.
40. J. Lindsey, I. Schrieman, H. Hsu, P. Kearney, A. Marguerettaz, *J. Org. Chem*. 1987, **52,** 827-836.

41. N. Ono, H. Hironaga, K. Simizu, K. Ono, K. Kuwano, T. Ogawa, *J. Chem. Soc*., *Chem. Commun.* 1994, 1019. N. Ono, H. Hironaga, K. Ono, S. Kaneko, T. Murashima, T. Ueda, C. Tsukamura, T. Ogawa. *J. Chem. Soc., Perkin Trans. 1* 1996, 417.
42. E.T. Pelkey, L. Chang, G.W. Gribble, *Chem. Commun.* 1996, 1909. E.T. Pelkey. G.W. Gribble. *Chem. Commun.* 1997, 1873. E.T. Pelkey, G.W. Gribble, *Synthesis* 1999, 1117.
43. T.D. Lash, C. Wijesinghe, A.T. Osuma, J.R. Patel, *Tetrahedron Lett.* 1997, **38,** 2031.
44. A. Adler, F. Longo, J. Finarelli, J. Goldmacher, J. Assour, L. Korsakoff, *J. Org. Chem*. 1967, **32**, 476.
45. Z. Assefa, A. Vantieghem, W. Deelereq, P. Vandenabeele, J.R. Vandenheede, W. Merlevede, P. de Witte, P. Agostinis, *J. Biol. Chem.* 1999, **274**, 8788-8796.
46. LG. Marzilli, *New J. Chem*. 1990, **14**, 409.